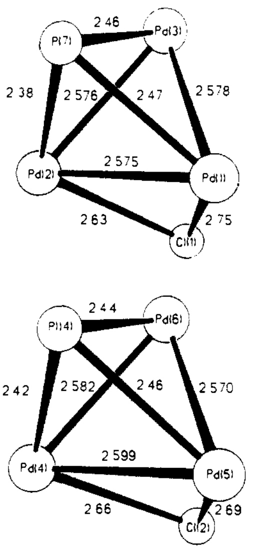

Figure 2. Dimensions within the cores of the two independent cations of $[(\mu\text{-}F_3P)Pd_3(\mu\text{-dpm})_3(\mu\text{-Cl})][PF_6]\cdot 0.5CH_2Cl_2$. In cation A (top) the Pd(3)···Cl(1) distance is 3.13 (1) Å, the P(4)–F distances (Å) are 1.59 (2) (F(1), 1.60 (2) (F(2)), and 1.61 (3) (F(3)), and the Pd–P(dpm) distances range from 2.31 (1) to 2.35 (1) Å. In cation B (bottom) the Pd(6)···Cl(2) distance is 2.96 (1) Å, the P(14)–F distances (Å) are 1.57 (3) (F(4)), 1.56 (2) (F(5)), and 1.64 (2) (F(6)), and the Pd–P(dpm) distances range from 2.28 (1) to 2.34 (1) Å. The Pd–P–Pd angles at the bridging PF_3 group are in the 63.0 (3)–64.4 (3)° range while the F–P–F angles span the range 91 (1)–93 (1)°. The esd's on the Pd–Pd distances are 0.004 Å, on the Pd–P distances 0.01 Å, and on the Pd–Cl distances 0.01 Å.

partially reversible. Removal of phosphorus trifluoride from a reaction solution in which only **2** and **3** are present allows **1** to reform as shown by ^{31}P NMR experiments.

The structure of the brown cluster has been determined by X-ray crystallography. There are two independent cationic clusters within the asymmetric unit; both have very similar dimensions. The structure of one is shown in Figure 1. Figure 2 shows some important dimensions within the PPd_3Cl core of both cations. The structure of each consists of a nearly equilateral triangle of palladium ions capped by the triply bridging phosphorus atom. The phosphorus atom is 1.93 Å out of the Pd_3 plane in both cations. A chloride ligand is unsymmetrically placed on the opposite face with relatively long Pd–Cl distances. This asymmetry is much greater in cation A than in cation B. While the position of this chloride bridge lowers the symmetry of the cluster, the F_3PPd_3 core very nearly has C_{3v} symmetry with a very narrow range of Pd-Pd distances (2.576-2.599 Å) and Pd-P distances (2.38-2.47 Å). The fluorine atoms of the PF_3 group are staggered over the Pd_3 plane. The structure is closely related to those of two palladium clusters with a triply bridging carbon monoxide, $[(\mu_3\text{-OC})Pd_3(\mu\text{-dpm})_3]^{2+}$ (**4**), and its halide ion adduct, $[(\mu_3\text{-OC})Pd_3(\mu\text{-dpm})_3(\mu\text{-Cl})]^+$ (**5**).[8] The Pd-Pd distances in **2** fall in the range seen for the typical single bonds in **4** (2.576 (1)-2.610 (1) Å),[9] **5** (2.584 (1)-2.603 (1) Å),[8] and $Pd_2(\mu\text{-dpm})_2Br_2$ (2.699 (1) Å).[10] As might be expected, the Pd-P distances to the triply bridging trifluorophosphine are slightly longer (by approximately 0.1 Å) than the Pd-P distances that are involved in bonding to the dpm ligands (which fall in the 2.28 (1)-2.35 (1) Å range). The Pd-P distances are also longer than the M-P distances in comparable terminal trifluorophosphine complexes (2.23 (1) Å for Pt-P in $Pt(PF_3)_4$;[11] 2.141 (2) Å for Pt-P in $PtCl_2(PEt_3)(PF_3)$[12]).

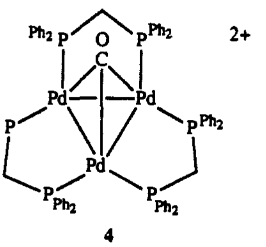

4

This observation of bridging by a simple phosphine introduces a new structural element into the chemistry of phosphorus(III) ligands and suggests that studies, such as those of phosphorus trifluoride binding to metal surfaces,[13] may need reevaluation since a basic assumption, that phosphorus trifluoride will confine itself to terminal coordination sites, is no longer valid. Further studies of bridging by group 15 ligands are in progress; doubly bridged complexes are a clear target.

Acknowledgment. We thank the National Science Foundation (CHE-8941209) for support and Johnson-Matthey, Inc., for a loan of palladium salts.

Supplementary Material Available: Views of the two cations and tables of atomic positional parameters, bond distances, bond angles, anisotropic thermal parameters, hydrogen atom positions, and data collection parameters for $[(\mu_3\text{-}F_3P)Pd_3(\mu\text{-dpm})_3(\mu\text{-Cl})](PF_6)\cdot 0.5CH_2Cl_2$ (17 pages); listing of observed and calculated structure factors for $[(\mu_3\text{-}PF_3)Pd_3(dpm)_3Cl]PF_6$ (56 pages). Ordering information is given on any current masthead page.

---

(8) Manojlović-Muir, L.; Muir, K. W.; Lloyd, B. R.; Puddephatt, R. J. *J. Chem. Soc., Chem. Commun.* **1985**, 536.

(9) Manojlović-Muir, L.; Muir, K. W.; Lloyd, B. R.; Puddephatt, R. J. *J. Chem. Soc., Chem. Commun.* **1983**, 1336.

(10) Holloway, R. G.; Penfeld, B. R.; Cotton, R.; McCormick, M. J. *J. Chem. Soc., Chem. Commun.* **1976**, 485.

(11) Marriot, J. C.; Salthouse, J. A.; Ware, M. J.; Freeman, J. M. *J. Chem. Soc., Chem. Commun.* **1970**, 595.

(12) Hitchcock, P. B.; Jacobson, B.; Pidcock, A. *J. Chem. Soc., Dalton Trans.* **1977**, 2043.

(13) Nitschke, F.; Ertl, G.; Kuppers, J. *J. Chem. Phys.* **1981**, *74*, 5911. Hoh, H.; Ertl, G. *Z. Naturforsch., A* **1982**, *37*, 346.

C–O Bond Scission in Heterometallic Alkoxides: Formation and Structure of $K_4Zr_2O(O^iPr)_{10}$

Brian A. Vaartstra, William E. Streib, and
Kenneth G. Caulton*

Department of Chemistry and
Molecular Structure Center
Indiana University, Bloomington, Indiana 47405

Received August 3, 1990

Efforts[1-3] to produce solid materials $M_aM'_bY_y$ and $M_aM'_bM''_cY_x$ from "molecular precursors" ($M_aM'_bX_m$ and $M_aM'_bM''_cX_n$, respectively, where X = R, OR, NR, NR_2, etc.) must focus on the *mechanism* of the transformation from molecule to infinite solid lattice if the performance of the resulting solid material is to be optimized. Such transformations could be envisioned to occur by low-energy hydrolysis (if Y = O), ammonolysis (if Y = N), but also higher energy bond scission processes due to pyrolysis, photolysis, or electrolysis. Scission of O–C bonds in particular (e.g., $M(OR)_n \rightarrow OM(OR)_{n-2} + \ldots$) is a procedure that is not yet under rational control, in part for lack of mechanistically detailed examples. We report here a contribution to this problem: the observation of C–O bond cleavage under very mild conditions, as well as the production of some new heterometallic alkoxides with noteworthy structures and solubility properties.

Reaction of equimolar $Zr_2(O^iPr)_8(^iPrOH)_2$ with KH in THF (or pentane) yields $KZr_2(O^iPr)_9$ (with release of 1 mol of PrOH and 1 mol of H_2) as an extremely pentane soluble product.[4] The

---

(1) Hubert-Pfalzgraf, L. G. *New J. Chem.* **1987**, *11*, 663.

(2) Bradley, D. C. *Chem. Rev.* **1989**, *89*, 1317.

(3) Caulton, K. G.; Hubert-Pfalzgraf, L. G. *Chem. Rev.* In press.

0002-7863/90/1512-8593$02.50/0

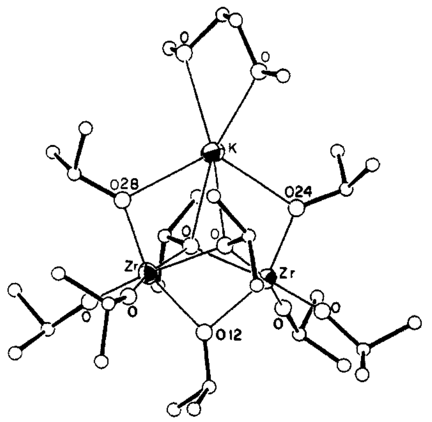

Figure 1. ORTEP drawing of non-hydrogen atoms of $KZr_2(O^iPr)_9$-$(MeOC_2H_4OMe)$. Unlabeled atoms are carbon. Average distances (Å): K–(μ_3-O) = 2.744 (8): K–(μ_2-O) = 2.722 (9); K–O_{ether} = 2.774 (9); Zr–(μ_3-O) = 2.224 (7), Zr–O12 = 2.203 (8); Zr–024 or 28 = 2.016 (8); Zr–O_{term} = 1.945 (9).

^1H and ^{13}C NMR spectra[5] of this compound in C_6D_6 at 25 °C are wholly consistent with C_{2v} symmetry as shown in structure I.[6] While this material is so soluble that we have been unable to grow crystals in nondonor solvents, we have been able to determine the structure of crystals grown from DME-$(MeOC_2H_4OMe)$/pentane.[7] As shown in Figure 1, the structure of this ether adduct is consistent with our assumed structure I. The NMR of this DME adduct is consistent with the symmetry of the DME-free compound.

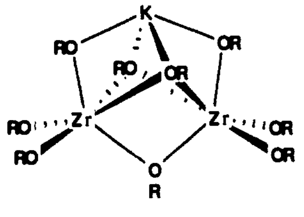

I

Given the presence of two hydroxyl functionalities in $Zr_2(O^iPr)_8(^iPrOH)_2$, we proceeded to react it with an additional equivalent (2 mol) of KH (in THF at 25 °C). This results in formation of compound I, together with a new species that displays (^1H and ^{13}C NMR) only two kinds of O^iPr groups in a 1:4 ratio. The solid-state structure of this pentane-soluble material[8] reveals the molecular species $K_4Zr_2O(O^iPr)_{10}$ (Figure 2). It is composed of a K_4Zr_2 octahedron (Zr's are trans) encapsulating a μ_6-O^{2-} unit. The eight triangular faces of the octahedron each carry a μ_3-O^iPr group. The sixth ligand on each Zr is a terminal isopropoxide. Most remarkable is the square-pyramidal coordination geometry of each K; in order for the K–(μ_6-O) distance (2.797 Å) to be similar to the K–O^iPr distance (2.736 Å average), K^+ protrudes outside of the square base of four oxygens, away from μ_6-O^{2-}. This has the consequence of leaving greater than one hemisphere around potassium naked, which is clearly shown in a space-filling representation. The exceptional capacity of the unit $Zr_2O(O^iPr)_{10}{}^{4-}$ to bind K^+ prompts our current effort to study its selectivity for alkali metal and alkaline earth cations.

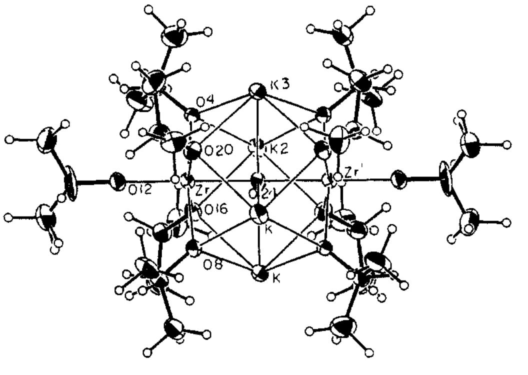

Figure 2. ORTEP drawing of $K_4Zr_2O(O^iPr)_{10}$, showing selective atom labeling. A center of symmetry at O24 generates the unlabeled atoms. Average distances (Å): K–(μ_3-O) = 2.736, K–(μ_6-O) = 2.797, Zr–(μ_3-O) = 2.127, Zr–O_{term} = 2.004, Zr–(μ_6-O) = 2.044. Average angle (μ_6-O)–K–(μ_3-O) = 61.68°.

To establish that the oxygen in this product was not derived from impurities in the KH (e.g., KOH), the above deprotonation was carried out with 2 equiv of $KN(SiMe_3)_2$. This gave the same product, $K_4Zr_2O(O^iPr)_{10}$.

The fate of the $CHMe_2$ group which is liberated on oxide abstraction to form $K_4Zr_2O(O^iPr)_{10}$ was of interest, particularly since literature reports of unexpected metal–oxo formation generally leave this question unanswered. Answering this question is complicated by the fact that considerable $KZr_2(O^iPr)_9$ is evident in all reactions that yield some $K_4Zr_2O(O^iPr)_{10}$ and the product ratio varies with the amount of KH or $KN(SiMe_3)_2$ employed. Thus, a balanced equation for a selective, high-yield synthesis of $K_4Zr_2O(O^iPr)_{10}$ by double deprotonation of $Zr_2(O^iPr)_8(^iPrOH)_2$ cannot be offered. Adventitious water (or hydroxide) or oxide extraction from the glassware seem unlikely as the sole source of the oxide since $K_4Zr_2O(O^iPr)_{10}$ is formed (although in reduced yield) when the reaction is repeated with glassware which has been silylated[9] and subsequently flame-dried under vacuum. The identities of the organic products produced along with $K_4Zr_2O(O^iPr)_{10}$ were established by reaction of KH with $Zr_2(O^iPr)_8(^iPrOH)_2$ in silylated glassware, followed by vacuum transfer and 500-MHz ^1H NMR analysis of the volatiles. This revealed propane, isopropyl alcohol, and a trace of acetone. Propene and $^iPr_2O$ are *not* produced. The small yield of acetone suggests that reduction-resistant (electropositive) high-valent metals can be reluctant to participate in the β-hydrogen shift process exhibited by the electron-rich alkoxide compounds of the later transition metals in low oxidation states.[10,11] When this experiment is repeated with KD, the propane is exclusively C_3H_8. We conclude from this experiment that KH (or KD) is not effecting nucleophilic heterolysis of the O–$CHMe_2$ bond. $K_4Zr_2O(O^iPr)_{10}$ is also among the products formed by addition of $3KO^iPr$ to $KZr_2(O^iPr)_9$; propane and acetone are also evident in this reaction. Since this reaction proceeds through $KZr_2(O^iPr)_9$, we suggest that oxide abstraction may occur at the μ_3-O^iPr group.[12]

Additional C–O bond scission occurs at higher temperatures. $K_4Zr_2O(O^iPr)_{10}$ sublimes under vacuum, but thermolysis of the bulk solid in a helium flow gives a sharp (260–300 °C) weight loss that may correspond to formation of a new solid composition: $K_4Zr_2O_5(O^iPr)_2$. This material shows no subsequent weight loss over a remarkably wide temperature range: 300–660 °C. This product, including the influence of the identity of the alkali metal on its formation, is currently under study.

---

(4) This material was previously prepared by another method. See: Bartley, W. G; Wardlaw, W. *J. Chem. Soc.* **1958**, 422.

(5) Selected NMR data: ^1H δ 1.2–1.6 (doublets, int = 1:2:2:2:2), $^{13}C\{^1H\}$ NMR δ 68–71 (*C*H, int = 4:1:2:2), δ 27–28.5 (*C*H_3, int. = 2:2:2:1:2).

(6) This structure is also adopted by $KU_2(O^tBu)_9$. See: Cotton, F. A.; Marler, O.; Schwotzer, W. *Inorg. Chem.* **1984**, *23*, 4211.

(7) Crystal data for $C_{31}H_{73}KO_{11}Zr_2$ at −131 °C: a = 21.190 (7) Å, b = 25.034 (8) Å, c = 12.535 (4) Å, α = 90.16 (2)°, β = 91.37 (2)°, γ = 91.92 (2)° with Z = 6 in space group $P\bar{1}$. There are three independent molecules in the asymmetric unit. $R(F)$ = 0.0824 and $R_w(F)$ = 0.0858 for 11 363 reflections with $I > 2\sigma(I)$.

(8) Crystal data for $C_{30}H_{70}K_4O_{11}Zr_2$ at −156 °C: a = 18.899 (2) Å, c = 12.931 (1) Å, Z = 4 in space group $P4_2/n$. The molecule sits on an inversion center. Intensity data were refined to $R(F)$ = 0.0568 and $R_w(F)$ = 0.0609.

(9) $Cl(Me_2SiO)_4Cl$, sold as "Surfasil" by Pierce Chemical Co.

(10) Bryndza, H. E.; Tam, W. *Chem. Rev.* **1988**, *88*, 1163.

(11) Hoffman, D. M.; Lappas, D.; Wierda, D. A. *J. Am. Chem. Soc.* **1989**, *111*, 1531.

(12) While we cannot rigorously exclude that *some* of the oxo group originates from adventitious O^{2-}, OH^-, or H_2O in some part of our apparatus, the detection of propane proves that some C–O scission occurs. Some of the hydrogen needed to form propane is accounted for by the acetone observed.

Acknowledgment. This work was supported by the National Science Foundation. We thank Scott Horn for skilled technical assistance.

Supplementary Material Available: Synthetic procedures, NMR spectral data, and atomic positional and thermal parameters for $KZr_2(O^iPr)_9(MeOC_2H_4OMe)$ and $K_4Zr_2O(O^iPr)_{10}$ (7 pages). Ordering information is given on any current masthead page.

Template-Directed Phenolic Oxidative Coupling. A Stereocontrolled Route to Spiro Dienones

James D. White,* Roger J. Butlin, Hoh-Gyu Hahn, and Alan T. Johnson

Department of Chemistry, Oregon State University Corvallis, Oregon 97331-4003

Received July 26, 1990

Intramolecular oxidative coupling of phenols is a reaction of pivotal importance in alkaloid biosynthesis,[1] but its efficient simulation, particularly in stereochemical terms, has been a vexing problem for chemical synthesis.[2] Recent studies directed toward stereocontrolled oxidative coupling of benzyltetrahydroisoquinolines[3] have focused on conformational constraints that enforce proximity on reacting phenolic rings,[4] and on chiral appendages[5] and catalysts[6] that induce asymmetry in the coupled product. We describe herein a strategy for asymmetric phenolic coupling that employs a chiral oxazolidine as template and leads to the spiro dienone enantiomer **8** with extraordinary efficiency (Scheme I).

The chiral educt (*R*)-(−)-arterenol (norepinephrine, **1**) was N-acylated with 3-[[4-[(*tert*-butyldimethylsilyl)oxy]phenyl]acetyl]thiazolidine-2-thione **2**[7] to yield amide **3** ($[\alpha]_D$ −25.2°).[8] After conversion to its methyl ether **4**, the hydroxy amide was treated with thionyl chloride and then with Hünig's base, to give oxazoline **6** ($[\alpha]_D$ +13.9°) with inverted configuration.[9] This stereochemical result is a consequence of participation by the amide function and, thus, retention of configuration[10] in the formation of the intermediate (unstable) chloride **5** ($[\alpha]_D$ −12.7°). The same configuration of **6** was obtained with *N*-chlorosuccinimide–dimethyl sulfide as halogenating agent.

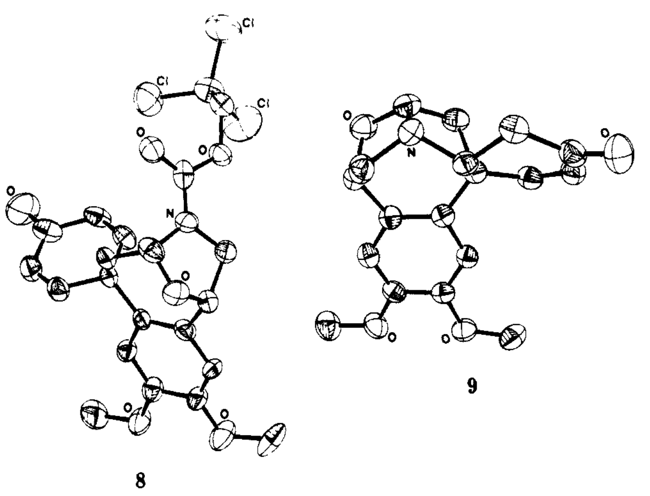

Figure 1. ORTEP plots of **8** and **9** with heteroatoms labeled. Thermal ellipsoids are drawn at the 50% level.

Scheme I[a]

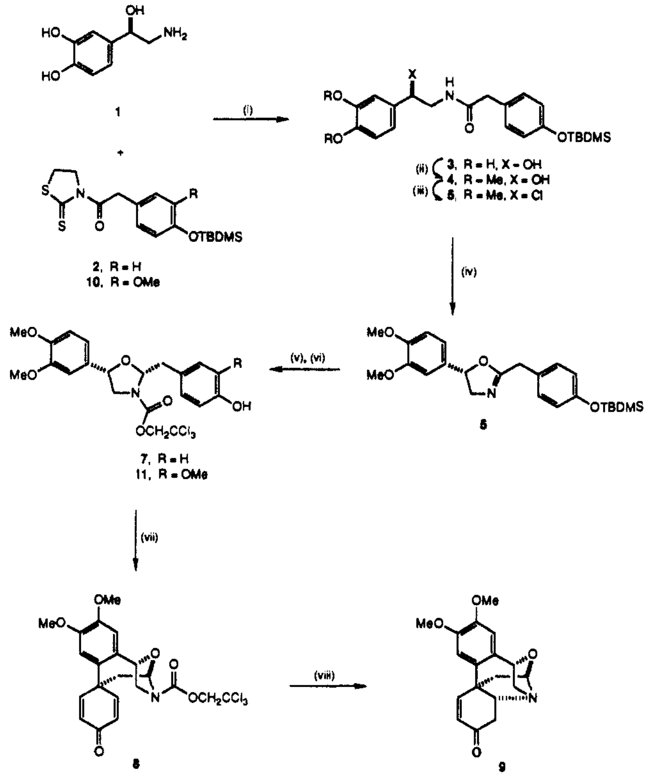

[a] (i) DMF, 25 °C, 82%; (ii) CH_2N_2, ether–MeOH, 25 °C, 100%; (iii) $SOCl_2$, CH_2Cl_2, 0 °C; (iv) i-Pr_2NEt, CH_2Cl_2, 82% from **4**; (v) Cl_3CCH_2OCOCl, THF, −78 °C, then $NaBH_3CN$, THF–EtOH, 65%; (vi) n-Bu_4NF, THF, 25 °C, 76%; (vii) VOF_3, $(CF_3CO)_2O$, TFA, CH_2Cl_2, −78 °C → −10 °C, 98%; (viii) Zn, MeOH, reflux, 50%.

Oxazoline **6** was acylated with 2,2,2-trichloroethyl chloroformate, and the intermediate salt was reduced with sodium cyanoborohydride to afford a mixture of cis and trans oxazolidines (3:1, respectively).[11] The mixture was subjected to tetra-*n*-butylammonium fluoride, furnishing the free phenols, which were separated chromatographically. The aryl rings in cis (2*R*,5*S*) isomer **7** ($[\alpha]_D$ +31.8°) are oriented in a manner that makes para–para coupling highly favorable, and when **7** was oxidized with vanadium oxytrifluoride[12] and trifluoracetic anhydride in a mixture of trifluoroacetic acid and dichloromethane, crystalline spiro dienone **8** ($[\alpha]_D$ +33.8°) was produced in quantitative yield.[13] The structure of **8** was established by means of an X-ray crys-

---

[1] Battersby, A. R. In *Oxidative Coupling of Phenols*; Battersby, A. R., Taylor, W. I., Eds.; Dekker: New York, 1967; pp 119–165.

[2] (a) Dhingra, O. P. In *Oxidation in Organic Chemistry*; Trahanovsky, W. S., Ed.; Academic Press: New York, 1982; Vol. 5-D, pp 207–278. (b) White, J. D.; Caravatti, G.; Kline, T. B.; Edstrom, E.; Rice, K. C.; Brossi, A. *Tetrahedron* **1983**, *39*, 2393 and references cited.

[3] Phillipson, J. D., Roberts, M. F., Zenk, M. H., Eds. *The Chemistry and Biology of Isoquinoline Alkaloids*; Springer-Verlag: Berlin, 1985. See also: Schwartz, M. A.; Pham, P. T. K. *J. Org. Chem.* **1988**, *53*, 2318 and references cited.

[4] Burnett, D. A.; Hart, D. J. *J. Org. Chem.* **1987**, *52*, 5662.

[5] Meyers, A. I.; Fuentes, L. M. *J. Am. Chem. Soc.* **1983**, *105*, 117. Meyers, A. I.; Fuentes, L. M.; Kubota, Y. *Tetrahedron* **1984**, *40*, 1361. Gawley, R. E.; Smith, G. A. *Tetrahedron Lett.* **1988**, *29*, 301.

[6] Noyori, R.; Ohta, M.; Hsiao, Y.; Kitamura, M.; Ohta, T.; Takaya, H. *J. Am. Chem. Soc.* **1986**, *108*, 7117 and references cited.

[7] Prepared from *p*-hydroxyphenylacetic acid by (i) protection with *tert*-butyldimethylsilyl chloride and imidazole in DMF, followed by workup with K_2CO_3 in aqueous MeOH, and (ii) exposure of the carboxylic acid to thiazolidine-2-thione, DCC, and DMAP in EtOAc (Burton, L. P. J.; White, J. D. *Tetrahedron Lett.* **1980**, *21*, 3147).

[8] Nagao, Y.; Kawabata, T.; Seno, K.; Fujita, E. *J. Chem. Soc., Perkin Trans. 1* **1980**, 2470.

[9] The absolute configuration of **6** was established by its hydrolysis to the enantiomer of **4** (cf: Meyers, A. I.; Hoyer, D. *Tetrahedron Lett.* **1985**, *26*, 4687).

[10] Pines, S. H.; Kozlowski, M. A. *J. Org. Chem.* **1972**, *37*, 292.

[11] When the reduction was carried out with sodium borohydride, the stereoselectivity was reversed.

[12] Kupchan, S. M.; Liepa, A. J. *J. Am. Chem. Soc.* **1973**, *95*, 4062.

[13] The oxidative coupling of **7** could also be accomplished with $VOCl_3$ and $PhI(OCOCF_3)_2$, but neither reagent approached the efficiency of VOF_3.

0002-7863/90/1512-8595$02.50/0